Available online at www.sciencedirect.com
ScienceDirect
Bioorganic & Medicinal Chemistry Letters
Bioorganic & Medicinal Chemistry Letters 17 (2007) 2874–2878

Design and evaluation of 'Linkerless' hydroxamic acids as selective HDAC8 inhibitors

Keris KrennHrubec,[a] Brett L. Marshall,[b] Mark Hedglin,[a] Eric Verdin[b] and Scott M. Ulrich[a,*]

[a]*Department of Chemistry, Ithaca College, Ithaca, NY 14850, USA*
[b]*Gladstone Institute of Virology and Immunology, University of California, San Francisco, CA 94158, USA*

Received 19 December 2006; revised 16 February 2007; accepted 21 February 2007
Available online 25 February 2007

Abstract—In this report, we describe new HDAC inhibitors designed to exploit a unique sub-pocket in the HDAC8 active site. These compounds were based on inspection of the available HDAC8 crystal structures bound to various inhibitors, which collectively show that the HDAC8 active site is unusually malleable and can accommodate inhibitor structures that are distinct from the canonical 'zinc binding group-linker-cap group' structures of SAHA, TSA, and similar HDAC inhibitors. Some inhibitors based on this new scaffold are >100-fold selective for HDAC8 over other class I and class II HDACs with IC_{50} values <1 μM against HDAC8. Furthermore, treatment of human cells with the inhibitors described here shows a unique pattern of hyperacetylated proteins compared with the broad-spectrum HDAC inhibitor TSA.

Post-translational ε-acetylation of lysine residues was first identified as a post-translational modification of histones and has since emerged as a central mechanism of transcriptional control in eukaryotes; hypoacetylation is correlated with transcriptional repression and hyperacetylation with transcriptional activation.[1–4] Patterns of lysine acetylation along regions of nucleosomes have distinct biological meanings, through recruitment of specific proteins as well as structural changes to the chromatin fiber.[5,6] Histone lysine acetylation patterns affect diverse cellular processes including differentiation, cellular response to stimuli, and tumorigenesis. More recently, it has been shown that non-histone proteins such as tubulin and p53 are also targets of reversible lysine acetylation, suggesting that acetylation may play a much broader role in controlling cellular events akin to protein phosphorylation.[7,8]

The lysine acetylation state of cellular proteins is determined by the action of histone acetyl transferases (HATs) and histone deacetylases (HDACs). There are three classes of HDACs. Class I (HDACs 1, 2, 3, and 8) and class II (HDACs 4, 5, 6, 7, 9, and 10) HDACs are zinc-dependent amidohydrolases with a conserved catalytic core but differing in size, domain structure, and tissue expression pattern. Class III HDACs are NAD+ dependent, unrelated in sequence and mechanism to classes I and II.[9] Zinc-dependent HDACs have received much attention as anticancer drug targets. Inhibitors of these enzymes have demonstrated a remarkable ability to induce terminal differentiation of transformed cells, presumably by altering patterns of gene expression through influencing the acetylation state of select histone lysine residues.[10] HDAC inhibitors are also exceedingly useful tools to study the biology of histone deacetylases. Indeed, determining whether a cellular process involves HDACs is readily ascertained by using the many potent, cell-permeable molecules available.

Most HDAC inhibitors such as TSA and SAHA closely resemble the aliphatic acetyl-lysine substrate and deliver a hydroxamic acid or other zinc binding group to the catalytic zinc ion at the bottom of a narrow active site pocket as seen in co-crystal structures of inhibited HDLP (HDAC-like protein),[11] HDAH (HDAC-like amidohydrolase),[12] and human HDAC8.[13] These inhibitors all have a zinc binding group and a polar 'cap

Keywords: Histone deacetylases; Hydroxamic acids; HDAC8.
* Corresponding author. Tel.: +1 607 274 7977; fax: +1 607 274 8135; e-mail: sulrich@ithaca.edu

0960-894X/$ - see front matter © 2007 Elsevier Ltd. All rights reserved.
doi:10.1016/j.bmcl.2007.02.064

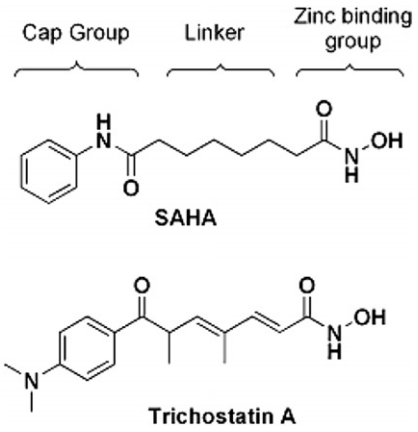

Figure 1. Common structural features of the broad-spectrum HDAC inhibitors SAHA and TSA.

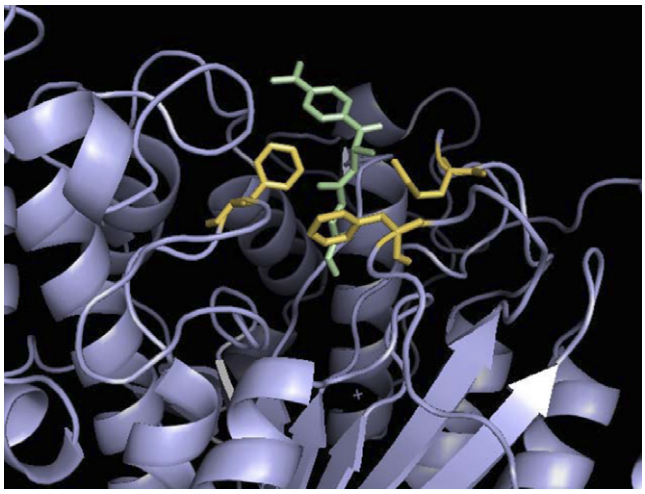

Figure 2. The HDAC8:TSA co-crystal structure, showing the conserved hydrophobic residues (F152, F208, and M274) that form the narrow active site channel, at the bottom of which is the catalytic zinc ion.

group' connected by a straight chain alkyl, vinyl or aryl linker (Fig. 1). Attempts to generate isozyme-specific HDAC inhibitors generally focus on varying the cap group to exploit variability in the HDAC surface surrounding the active site.[14] Despite much effort, truly selective compounds remain difficult to find. Screens of large compound libraries have yielded selective inhibitors of HDACs 1, 6, and 8.[15,16] However, structural determinants of selective HDAC inhibition remain unknown. In this report, we describe the rational design of HDAC inhibitors which show selectivity toward human HDAC8 by targeting an active site pocket which may be unique to this family member.

HDAC8 is an unusual HDAC family member. Recent data suggest that HDAC8 is constitutively localized to the cytoplasm and its expression in primary cells is restricted to smooth muscle.[17] Interestingly, RNAi ablation of HDAC8 in these cells results in a contraction-deficient phenotype.[18] Thus, identifying the substrates of HDAC8 may expand the range of targets and functions of the HDAC family. Furthermore, a common form of acute myeloid leukemia (AML) results from a chromosomal translocation creating an abnormal fusion protein, Inv1. Inv1 binds HDAC8 and is associated with aberrant, constitutive genetic repression.[19] As such, specific HDAC8 inhibitors may assist a medicinal chemistry effort against AML.

Our approach to generate specific HDAC8 inhibitors is founded upon analysis of the HDAC8, HDAH, and HDLP structures with bound hydroxamate inhibitors. The amino acid sequences and overall active site topology of the enzymes are similar. In HDAC8, the zinc ion that facilitates amide hydrolysis is found at the bottom of a narrow pocket; just above which are conserved and catalytically important Y306 and H180 residues. The rim of the pocket is formed by three conserved hydrophobic residues, F152, F208, and M274 (Fig. 2). These form the tunnel that the acetyllysine substrate and straight-chain hydroxamate inhibitors penetrate to access the catalytic machinery. Similar architecture is found in HDLP and HDAH.

The HDAC8 structure was solved with four different hydroxamate inhibitors bound.[13] The active site topology of HDAC8 showed large structural differences depending on which inhibitor is bound. In the SAHA:HDAC8 co-crystal structure, the active site is deep and narrow similar to the HDLP and HDAH structures. However, when a hydroxamate inhibitor with an aryl linker (CRA-A) is bound to HDAC8, a large sub-pocket forms in the side of the active site, adjacent to M274. This pocket is created by movement of F152 away from its normal position packed against M274 to form the lip of the active site tunnel (Fig. 3). This shift may be a consequence of the more sterically demanding aryl hydroxamate CRA-A versus the aliphatic hydroxamate SAHA binding the active site.

We reasoned that this sub-pocket may be targeted by a new inhibitor scaffold. If this pocket is unique to HDAC8, inhibitors that bind this pocket should be selective for HDAC8. To test this idea, we synthesized a panel of six bulky aryl hydroxamic acids that are unlike the canonical 'zinc binding group-linker-cap group' structure of most HDAC inhibitors (Fig. 4). These inhibitors are aryl hydroxamates like CRA-A and the new scaffold also displays aryl groups to bind this pocket a short distance from the hydroxamic acid. Such molecules should be excluded from HDACs that lack the sub-pocket seen in HDAC8.

Compounds **1**–**6** were synthesized in two steps from the corresponding carboxylic acids by conversion to the acid chlorides followed by treatment with hydroxylamine in water/THF under basic conditions and purified by recrystallization from ethanol/water.[20] To access structure **6**, we first performed a Suzuki coupling between 1-naphthyl boronic acid and *p*-bromobenzoic acid to make *p*-(1-naphthyl)benzoic acid which was converted to its corresponding hydroxamate in the same manner (Scheme 1). All hydroxamates gave ^{1}H and ^{13}C NMR spectra consistent with the structures shown.[21] The

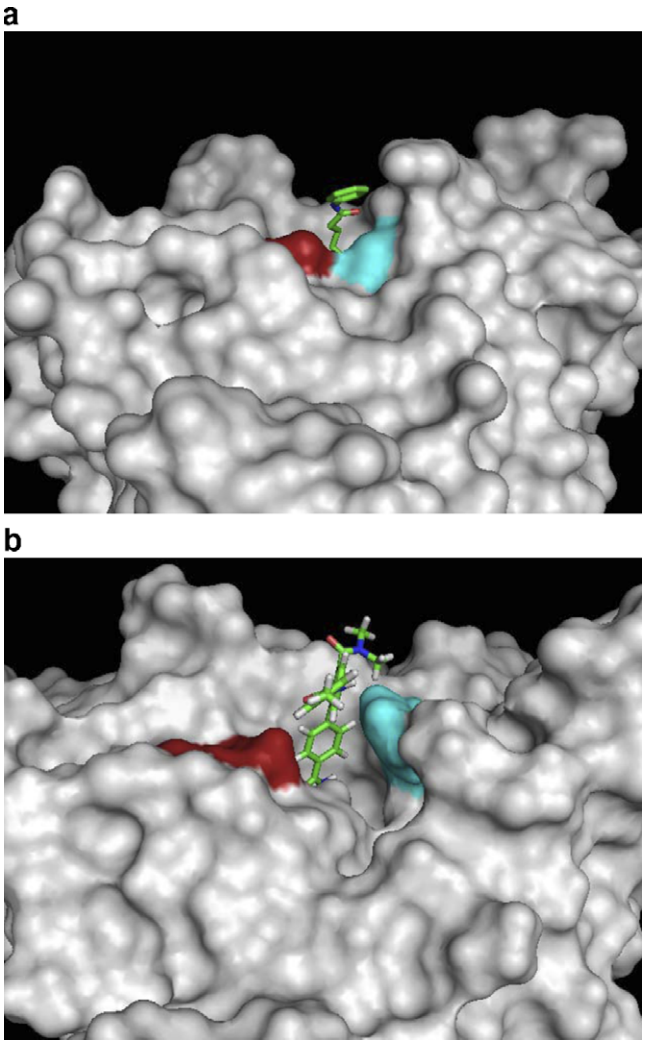

Figure 3. (a) Structure of HDAC8 bound to SAHA, an alkyl-linker HDAC inhibitor. M274 (red) and F152 (cyan) pack against each other to form the wall of the active site pocket. (b) Structure of HDAC8 bound to CRA-A, an aryl-linker HDAC inhibitor. In this case F152 rotates away from M274, exposing a large sub-pocket.

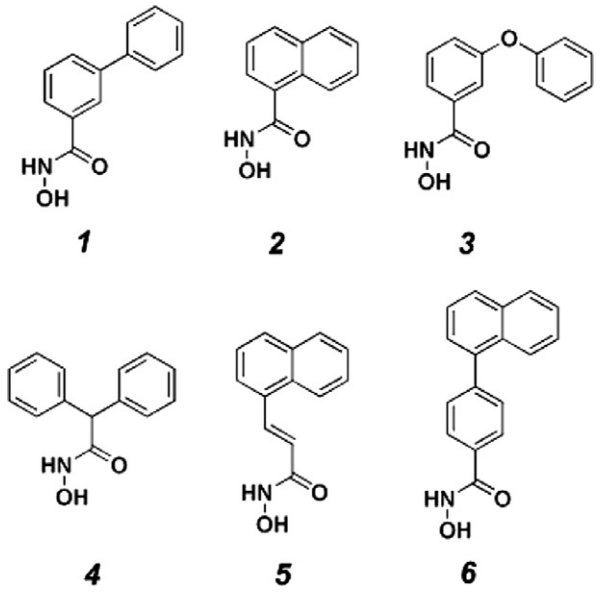

Figure 4. Structures of linkerless hydroxamates designed to bind the sub-pocket of the HDAC8 active site.

Table 1. IC_{50} values of compounds **1**–**6** against HDACs 1, 6, and 8

Compound	IC_{50} values		
	HDAC8(μM)	HDAC1(μM)	HDAC6(μM)
1	20.0	>100	>100
2	14.0	>100	>100
3	6.6	—	—
4	66.0	—	—
5	0.7	>100	82
6	0.3	>100	55

Values are the average of three experiments.

compounds were then tested as HDAC inhibitors using a tritiated acetyl histone peptide assay[22] against recombinant human HDAC8. The selectivity of the compounds was determined by similar inhibition assays against immunoprecipitated human HDACs 1 (class I) and 6 (class II) as representatives of the larger family.

The inhibition data show that the linkerless, sterically demanding aryl hydroxamates are indeed HDAC8 inhibitors (Table 1 and Fig. 5). Some of the compounds are also moderately potent; compounds **5** and **6** have submicromolar IC_{50} values against HDAC8. We also tested compounds **1**, **2**, **5**, and **6** as inhibitors against HDACs 1 and 6 to determine their selectivity toward HDAC8. The data show that all hydroxamates based on the linkerless scaffold are selective for HDAC8 over HDACs 1 and 6. The most potent compounds **5** and **6** are >100-fold selective against HDAC8 versus HDACs 1 and 6. The less potent compounds may be even more so, since they present steric bulk in closer proximity to the zinc binding group, potentially clashing with the narrow active site seen in HDAH and HDLP.

We designed compounds **1**–**6** based on a simple blocking effect, where the malleability of the HDAC8 active site with the inducible sub-pocket would allow the bulky hydroxamates to access the catalytic zinc while HDACs with more rigid, narrow active sites prohibit zinc chelation. Inspection of the CRA-A:HDAC8 co-crystal structure reveals that the primary pocket between F152 and F208 where the aryl group bearing the hydroxamate binds is at a right angle to the induced sub-pocket

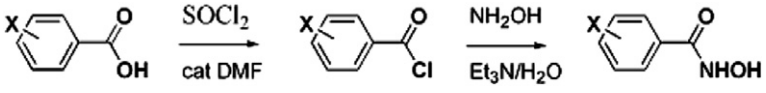

Scheme 1. Synthesis of hydroxamates shown in Figure 4. Crude acid chlorides were not isolated, and yields from the starting carboxylic acids were >80%.

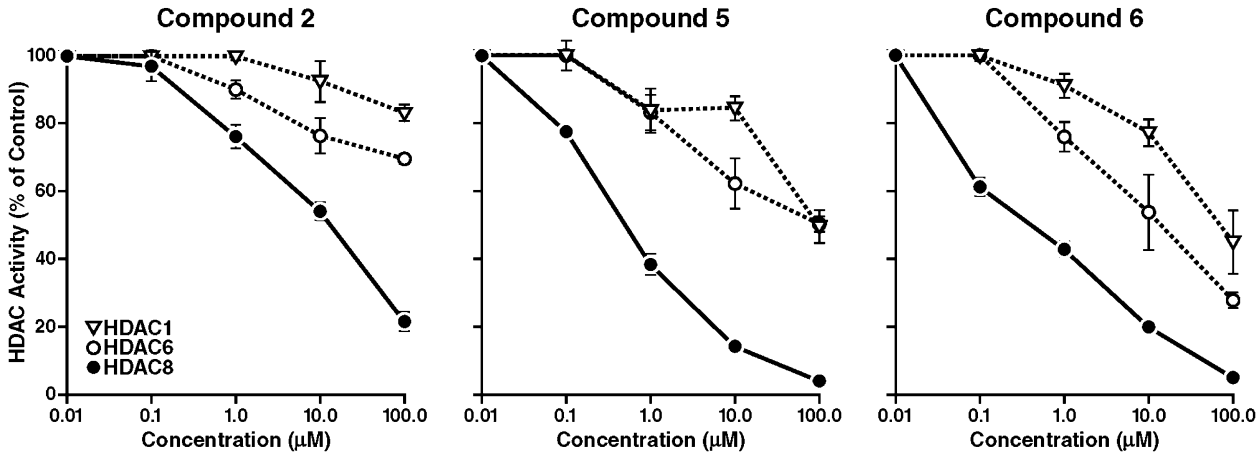

Figure 5. Inhibition plots of compounds **2, 5**, and **6** against HDACs 1, 6, and 8.

(Fig. 6). Interestingly, the more potent molecules against HDAC8 (**5** and **6)** have such conformations accessible to them, which may explain why the conformationally rigid compounds **1**–**4** are poorer inhibitors of HDAC8 than compounds **5** and **6**.

In order to determine the effects of these compounds on the levels of lysine acetylated proteins in cells, we treated HeLa and HEK293 cells with compounds **2**, **5** and the broad-spectrum HDAC inhibitor TSA. The cell lysate was then subjected to western blotting with anti-acetyl-lysine antibodies (Fig. 7). The data show that treating either cell type with TSA increased the lysine acetylation level of three proteins. The same three proteins became hyperacetylated upon treatment with compound **5**. While compound **5** does show selectivity among purified HDACs 1, 6, and 8, it has nearly identical effects on protein acetylation levels in cells as TSA. Thus, it is likely that compound **5** has targets among the HDAC family that we have not included in our selectivity assay. However, when either cell type was treated with compound **2**, only the high molecular weight protein became hyperacetylated. The high molecular weight protein was determined to be tubulin when the experiment was repeated with antibodies specific toward acetyl tubulin and acetyl histone (Fig. 8). HDAC6 has previously been shown to deacetylate tubulin specifically.[8] Our data show that compound **2** weakly inhibits HDAC6, which would account for this result, but tubulin hyperacetylation is seen at concentrations of **2** (0.8 μM) that showed minimal inhibition of purified HDAC6. These data do, however, clearly indicate that compound **2** inhibits a restricted subset of HDACs (possibly only HDAC8) in cells when compared with TSA, and the target(s) of compound **2** do not deacetylate histones. Rather, the target(s) of compound **2** deacetylate tubulin and possibly other non-histone proteins.

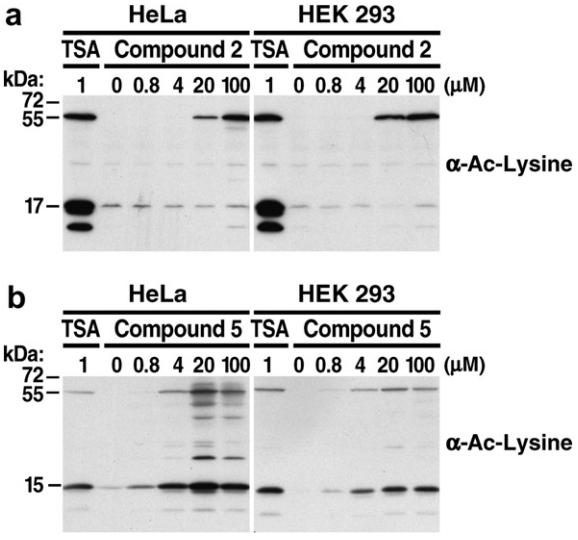

Figure 7. Anti-acetyl lysine Western blot of HeLa and HEK293 cell lysates pretreated with TSA (relatively nonspecific HDAC inhibitor), no inhibitor, and increasing concentrations of compounds **2** and **5**.

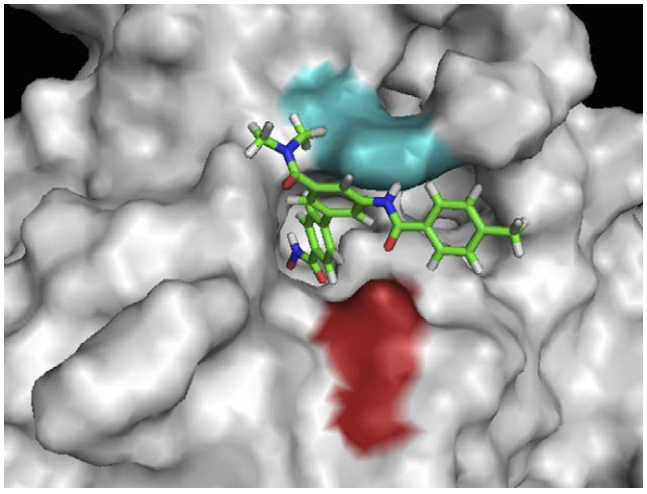

Figure 6. The HDAC8 CRA-A co-crystal structure showing the right-angle orientation of the aryl linker relative to the induced sub-pocket. Note that the aryl group of CRA-A attached to the aryl linker does not bind the sub-pocket but rather is positioned well above it, as can be seen in Figure 3b.

These compounds represent rationally designed inhibitors specific for an individual HDAC family member

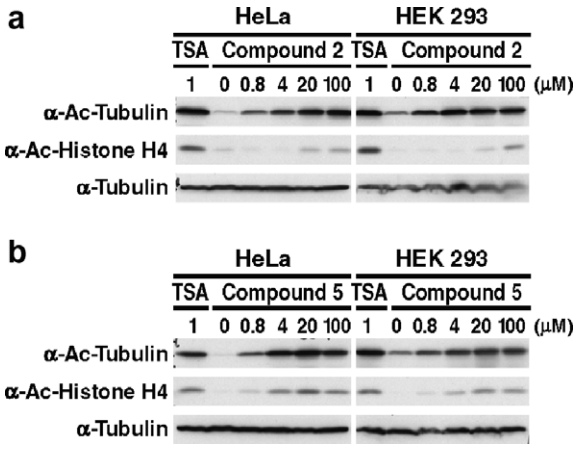

Figure 8. Western blotting of the same lysates with antibodies specific for lysine acetylated histone H4 and lysine acetylated tubulin.

based on available structural data. We hypothesize that the relatively simple structures described here exploit the malleability of the HDAC8 active site and its unique sub-pocket, resulting in selective inhibition. As more HDAC family members are structurally characterized, it will be seen if HDACs that are insensitive to these compounds also lack the sub-pocket seen in HDAC8. If so, this may emerge as a general structural feature that can be exploited to generate selective inhibitors. The compounds described here are also likely to serve as useful tools to study the role of HDAC8 in smooth muscle cell contraction, identify its protein targets, and serve as lead compounds for medicinal chemistry efforts against AML.

Acknowledgments

We thank Chris Roessler for early work on this project. Figures 2, 3, and 6 were generated with PyMol (Delano Scientific). This work was supported by the Research Corporation's Cottrell College Science Award #CC5955 (S.M.U.) and The Gladstone Institutes (E.V.).

Supplementary data

Supplementary data associated with this article can be found, in the online version, at doi:10.1016/j.bmcl.2007.02.064.

References and notes

1. Kornberg, R. D.; Lorch, Y. *Cell* **1999**, *98*, 285.
2. Jenuwein, T.; Allis, C. D. *Science* **2001**, *293*, 1074.
3. Peterson, C. L.; Laniel, M. A. *Curr. Biol.* **2004**, *14*, R546.
4. Struhl, K. *Gene Dev.* **1998**, *12*, 599.
5. Hecht, A.; Laroche, T.; Strahl-Bolsinger, S.; Gasser, S. M.; Grunstein, M. *Cell* **1995**, *80*, 583.
6. Shogren-Knaak, M.; Ishii, H.; Sun, J. M.; Pazin, M. J.; Davie, J. R.; Peterson, C. L. *Science* **2006**, *311*, 844.
7. North, B. J.; Marshall, B. L.; Borra, M. T.; Denu, J. M.; Verdin, E. *Mol. Cell* **2003**, *11*, 437.
8. Hubbert, C.; Guardiola, A., et al. *Nature* **2002**, *417*, 455.
9. Holbert, M. A.; Marmorstein, R. *Curr. Opin. Struct. Biol.* **2005**, *15*, 673.
10. Marks, P. A.; Richon, V. M.; Miller, T.; Kelly, W. K. *Adv. Cancer Res.* **2004**, *91*, 137.
11. Finnin, M. S.; Donigian, J. R.; Cohen, A.; Richon, V. M.; Rifkind, R. A.; Marks, P. A.; Breslow, R.; Pavletich, N. P. *Nature* **1999**, *401*, 188.
12. Nielsen, T. K.; Hildmann, C.; Dickmanns, A.; Schwienhorst, A.; Ficner, R. *J. Mol. Biol.* **2005**, *354*, 107.
13. Somoza, J. R.; Skene, R. J.; Katz, B. A.; Mol, C.; Ho, J. D.; Jennings, A. J.; Luong, C.; Arvai, A.; Buggy, J. J.; Chi, E.; Tang, J.; Sang, B. C.; Verner, E.; Wynands, R.; Leahy, E. M.; Dougan, D. R.; Snell, G.; Navre, M.; Knuth, M. W.; Swanson, R. V.; McRee, D. E.; Tari, L. W. *Structure* **2004**, *12*, 1325.
14. Sternson, S. M.; Wong, J. C.; Grozinger, C. M.; Schreiber, S. L. *Org. Lett.* **2001**, *3*, 4239.
15. Haggarty, S. J.; Koeller, K. M.; Wong, J. C.; Grozinger, C. M.; Schreiber, S. L. *Proc. Natl. Acad. Sci. U.S.A.* **2003**, *100*, 4389.
16. Hu, E. et al. *J. Pharmacol. Exp. Ther.* **2003**, *307*, 720.
17. Waltregny, D.; De Leval, L.; Glenisson, W.; Ly Tran, S.; North, B. J.; Bellahcene, A.; Weidle, U.; Verdin, E.; Castronovo, V. *Am. J. Pathol.* **2004**, *165*, 553.
18. Waltregny, D.; Glenisson, W.; Tran, S. L.; North, B. J.; Verdin, E.; Colige, A.; Castronovo, V. *FASEB J.* **2005**, *19*, 966.
19. Durst, K. L.; Lutterbach, B.; Kummalue, T.; Friedman, A. D.; Hiebert, S. W. *Mol. Cell. Biol.* **2003**, *23*, 607.
20. Summers, J. B.; Mazdiyasni, H.; Holms, J. H.; Ratajczyk, J. D.; Dyer, R. D.; Carter, G. W. *J. Med. Chem.* **1987**, *30*, 574.
21. Compound **2**: ^{1}H NMR (DMSO-d_6, 400 MHz) δ = 7.51 (m, 4H), 7.94 (m, 2H), 8.15 (m, 1H), 9.24 (s, 1H), 11.09 (s, 1H). ^{13}C NMR (DMSO-d_6, 100 MHz) δ = 166.18, 133.65, 132.77, 130.56, 128.79, 127.33, 126.87, 126.02, 125.71, 125.54 ppm.
Compound **5**: ^{1}H NMR (400 MHz, DMSO-d_{-6}) δ = 10.86 (s, 1H), 9.11 (s, 1H), 8.20 (d, J = 16 Hz, 1H), 7.95 (m, 2H), 7.77 (m, 1H), 7.60 (m, 4H), 6.55 (d, J = 16 Hz, 1H). ^{13}C NMR (100 MHz, DMSO-d_{-6}) δ = 163.11, 135.31, 133.85, 132.45, 131.26, 130.12, 129.21, 127.47, 126.79, 126.30, 124.94, 123.69, 122.76 ppm.
Compound **6**: ^{1}H NMR (400 MHz, DMSO-d_{-6}) δ = 11.32 (s, 1H), 9.11 (s, 1H), 7.97 (m, 4H), 7.75 (d, J = 7.4 Hz, 1H), 7.52 (m, 6H). ^{13}C NMR (100 MHz, DMSO-d_{-6}) δ = 164.54, 143.30, 139.16, 133.94, 132.33, 131.11, 130.34, 128.98, 128.60, 127.61, 127.52, 127.12, 126.60, 126.12, 125.55 ppm.
22. Verdin, E.; Dequiedt, F.; Fischle, W.; Frye, R.; Marshall, B.; North, B. *Methods Enzymol.* **2004**, *377*, 180.